Electronic Supplementary Material (ESI) for Environmental Science: Nano.

Supporting Information

Photochemical transformations of thiolated polyethylene glycol coatings on gold nanoparticles

Stacey M. Louie,[1] Justin M. Gorham,[1] Eric A. McGivney,[2,3] Kelvin B. Gregory,[2,3] Vincent A. Hackley[1*]

[1]Materials Measurement Science Division, National Institute of Standards and Technology (NIST), Gaithersburg, MD, 20899

[2]Center for the Environmental Implications of NanoTechnology (CEINT), Carnegie Mellon University, Pittsburgh, PA, 15213

[3]Department of Civil and Environmental Engineering, Carnegie Mellon University, Pittsburgh, PA, 15213

*Corresponding author

Phone: 301-975-5790

Email: vince.hackley@nist.gov

Address: 100 Bureau Dr., MS 8520, Gaithersburg, MD, 20899

Table of Contents

Table of Figures

Table of Tables

1. Materials

Reagents used for actinometry experiments include potassium ferrioxalate trihydrate ($K_3Fe(C_2O_4)_3 \cdot 3H_2O$) (Alfa Aesar, Ward Hill, MA),¶ 1,10-phenanthroline (>99%, Sigma Aldrich, St. Louis, MO), sodium acetate (ACS grade, Alfa Aesar, Ward Hill, MA), and sulfuric acid (HPLC grade, Fluka). Fluorescence experiments were performed using 5000 Da rhodamine-tagged polyethylene glycol thiol (RhPEGSH) (Nanocs, New York, NY), prepared at 1 g L^{-1} in deionized (DI) water. Reagents used for Ellman's assay include 5,5'-dithiobis-(2-nitrobenzoic acid) (DTNB or Ellman's reagent) (99%, Sigma Aldrich, St. Louis, MO), potassium phosphate monobasic (>99%, Fisher Scientific, Pittsburgh, PA), and potassium phosphate dibasic (ACS reagent grade, Sigma Aldrich, St. Louis, MO). Eluents for asymmetric flow field-flow fractionation (A4F) and liquid chromatography mass spectrometry (LC-MS) were prepared using ammonium nitrate (99.999%, Alfa Aesar, Lancashire, UK), ammonium acetate (>99.99%, Sigma Aldrich, St. Louis, MO; > 97%, Fisher Scientific, Pittsburgh, PA), ammonium hydroxide (LabChem, Pleasant Prairie, WI; Acros Organics, Geel, Belgium), and acetonitrile (HPLC grade, EMD Millipore, Billerica, MA). For photosensitizer experiments, reagents were sodium nitrate (ACS reagent grade, J.T. Baker, Center Valley, PA) and hydrogen peroxide (ACS reagent grade, J.T. Baker, Center Valley, PA). Sodium bicarbonate (molecular biology grade, Sigma Aldrich, ST. Louis, MO) was used in solutions for DLS and EPM measurements and indirect photochemistry experiments.

2. Ferrioxalate actinometry method and measurements

Actinometry experiments were performed following the "micro" method by Fischer.[1] A solution of 0.012 mol L^{-1} of potassium ferrioxalate was prepared in 0.05 mol L^{-1} H_2SO_4, and 3 mL aliquots were irradiated in quartz vials in the reactor. After irradiation, 0.5 mL of a 0.1 % mass fraction 1,10-phenanthroline solution (prepared in 0.5 mol L^{-1} H_2SO_4 with 3.1 g L^{-1} sodium acetate) was added, and the absorbance of the Fe^{2+}-phenanthroline complex was measured at 510 nm on a Lambda 750 spectrophotometer (Perkin Elmer, Waltham, MA). The rate of photon absorption by the 3 mL of irradiated solution was determined to be $\approx 5 \times 10^{16}$ s^{-1}. The irradiance was estimated to be ≈ 30 W m^{-2} around the cylindrical surface area of the liquid column, as calculated from the rate of total photon absorption and accounting for the spectral distribution of irradiance density reported by the manufacturer for the UV lamps (Southern New England Ultraviolet Co., Branford, CT).

3. Ellman's assay

Ellman's assay was performed by mixing 1 mL of sample with 0.2 mL of phosphate buffer (0.5 mol L^{-1}, pH 8) and 25 μL of DTNB solution (4 g L^{-1} in 0.08 mol L^{-1} phosphate buffer) and allowing 15 min for reaction. The reduced thiol concentration was quantified from the concentration of 5-thiobis-(2-nitrobenzoate) (TNB^-) ion, as determined from the UV-vis absorbance at 412 nm (Lambda 750 spectrometer).

¶ The identification of any commercial product or trade name does not imply endorsement or recommendation by the National Institute of Standards and Technology.

4. Asymmetric flow field-flow fractionation (A4F) setup and method

Table S1. A4F-UV-DLS settings

Sample concentration	≈ 9 mg L^{-1} AuNPs
Injection volume	100 μL
Spacer height	250 μm
Membrane	Polyethersulfone, 10 kDa molar mass cut-off
Mobile phase composition	0.5 mmol L^{-1} NH_4NO_3
Detector flowrate	0.5 mL min^{-1}
Cross flowrate	0.5 mL min^{-1}
Focus flowrate	2.0 mL min^{-1}
Fractionation method	0-1 min: Elution only 1-2 min: Focus 2-6 min: Focus + injection 6-31 min: Elution with cross-flow
Dynamic light scattering (DLS) detector settings	Measurement angle: 173° Measurement duration: 5 s Data analysis: Cumulants method (ISO 13321:1996)

5. Composition of moderately hard water (MHW) and artificial seawater (ASW)

The composition of the MHW used in the aggregation studies was 0.05 mmol L^{-1} KCl (4.0 mg L^{-1} KCl), 0.54 mmol L^{-1} $NaHCO_3$ (44.9 mg L^{-1} $NaHCO_3$), 0.35 mmol L^{-1} $MgSO_4$ (41.7 mg L^{-1} $MgSO_4$ (anhydrous)), and 1.4 mmol L^{-1} $CaCl_2$ (204 mg L^{-1} $CaCl_2{\cdot}2(H_2O)$). The composition of the ASW is provided in Table S2. After addition of the AuNP suspension, the final concentrations of salts in the ASW solution were 90% of those reported in Table S2.

Table S2. Composition of ASW (ASTM D 1141, without heavy metals)

Compound	Concentration (g L^{-1})	Concentration (mmol L^{-1})
NaCl	24.53	419.7
$MgCl_2$	5.20	54.6
Na_2SO_4	4.09	28.8
$CaCl_2$	1.16	10.5
KCl	0.695	9.32
$NaHCO_3$	0.202	2.40
KBr	0.101	0.849
H_3BO_3	0.027	0.437
$SrCl_2$	0.025	0.158
NaF	0.003	0.071

6. LC-MS sample preparation and run conditions

Methoxy polyethylene glycol thiol (mPEGSH) solutions and supernatants were reacted with DTNB within one day of sample collection and refrigerated. The DTNB reaction was performed in 1.6 mmol L^{-1} ammonium acetate in water (adjusted to pH 8 with ammonium hydroxide) to better match the LC-MS eluent composition. The primary purpose of the DTNB derivatization was to form a mixed disulfide species (mPEGS-TNB) in order to prevent disulfide formation between the free mPEGSH during the time between sample collection and LC-MS analysis. Underivatized samples were also analyzed.

Table S3. LC-MS Run Conditions

LC Conditions	
Column	Agilent Eclipse XDB-C18, 5um, 4.6 x 150 mm
Injection volume	5 µL, injection with needle wash in DI H2O
Mobile phase A	1 mmol L^{-1} ammonium acetate in water, pH 8
Mobile phase B	Acetonitrile
Solvent run type	Isocratic, 1:1 mixture of mobile phase A:B
Column temperature	22.0 °C
Flow rate	0.5 mL min^{-1}
MS Conditions	
Ion source	ESI
Scan type	MS2 Scan
Start mass	20 u
End mass	2000 u
Scan time	500 ms
Fragmentor voltage	250 V
Cell accelerator voltage	7 V
Polarity	Positive
Scan step size	0.1 u
Gas temperature	300 C
Gas flow	11 L min^{-1}
Nebulizer	15 psi (0.1034 MPa)
Chromatogram type	Total ion count (TIC)

7. X-ray Photoelectron Spectroscopy (XPS) analysis

Elemental percentages were acquired by fitting spectra with a Shirley baseline (with exception of the S(2p), which had a linear baseline), integrating, and adjusting the calculated area using manufacturer provided relative sensitivity factors (RSF) of 0.78, 0.278, 0.668, and 6.25 for the O (1s), C (1s), S (2p) and the Au (4f) regions, respectively. All AuNP containing spectra were adjusted to 83.9 eV representative of zero-valent Au[2] and the mPEG-SH controls were adjusted to 532.8 eV representative of the O (1s) peak maximum for the ether O.[3] To assess the distribution of S oxides relative to the overall S content, peak fitting analysis was performed on the S (2p) using Gaussian peaks with 30% Lorentzian tailoring. The S ($2p^{3/2}$) transition was set to >168 eV and the $2p^{1/2}$ transition was set to be 1.25 eV higher binding energy and was set to 50% of the signal intensity. While a set of peaks with all constraints kept constant were included for reduced S, they were used only to enable a good fit and not to model any particular chemical state. Therefore, all reported values for the S content are either reflective of the total S (2p) composition or the oxidized S (-SO$_x$) composition.

8. Batch UV-vis absorbance spectra

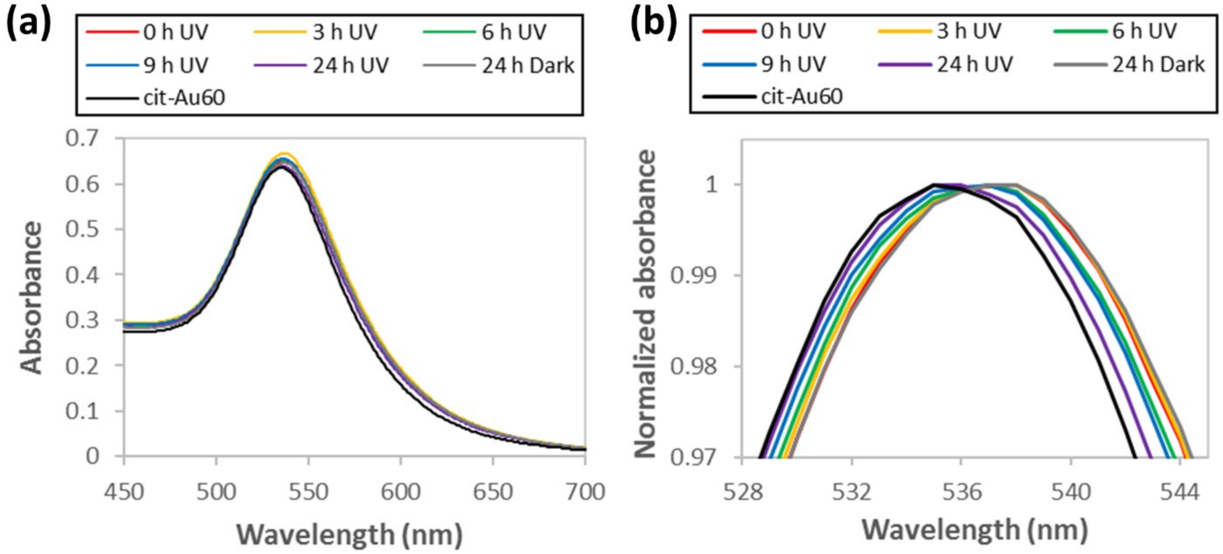

Figure S1. Batch UV-vis absorbance spectra for the Au-mPEGSH$_{5000}$ NPs show minimal change in the maximum absorbance (a) but a blue shift in the SPR peak (b) upon UV irradiation. The blue shift was observed reproducibly across three independent samples (not shown). Absorbances in (b) are normalized to the maximum absorbance for each sample for visual clarity. Au-mPEGSH$_{5000}$ NPs were prepared using the more highly reduced mPEGSH stock (with dithiothreitol (DTT) impurity).

9. Preparation of fluorescently tagged coatings and detection of desorbed fluorophore

AuNPs were prepared with fluorescent RhPEGSH coatings and are denoted Au-RhPEGSH. For adsorption to the NPs, a mixture of 25 mg L^{-1} RhPEGSH and 25 mg L^{-1} mPEGSH (5 kDa) was used because NPs coated solely with the positively-charged RhPEGSH exhibited aggregation upon washing. The coated NPs were rinsed four times by centrifugation in an Eppendorf Mini-Spin centrifuge (Eppendorf, Hauppauge, NY) at 14000 rpm (≈ 13150 *g*) and 23 °C for 3 min and resuspension of the AuNP pellet in DI water.

Supernatants of the pelleted Au-RhPEGSH NPs were collected in the dark and UV-exposed samples for detection of fluorophore that detached from the AuNP surface. Batch measurements were taken on an Agilent 1260 Infinity fluorescence detector on samples injected by syringe pump. Because of the wide bandwidth (20 nm) of the instrument, the peak excitation and emission wavelengths (λ_{ex} = 554 and λ_{em} = 579 nm, respectively) for rhodamine were not used to avoid scattering interferences from water. Rather, λ_{ex} = 250 nm and λ_{em} = 575 nm were used, and a linear dependence of fluorescence intensity with RhPEGSH concentration was confirmed for these settings.

The duration of UV exposure was 6 h, after which a significant decrease in the PEG layer thickness is observed but before the reaction reaches completion (Figure 2). A longer duration was not selected to minimize photobleaching of the rhodamine. Higher rhodamine fluorescence intensity in the supernatant of the UV-exposed Au-RhPEGSH NPs ((0.152 ± 0.009) lm, *n* = 3 samples) indicates greater detachment of rhodamine from the NPs compared to the dark control ((0.089 ± 0.011) lm, *n* = 3 samples); representative spectra are shown in Figure S2.

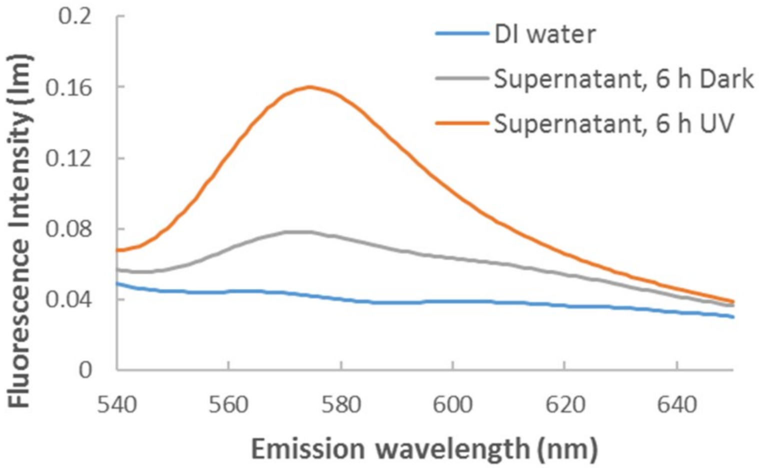

Figure S2. Representative fluorescence spectra for the supernatants containing unadsorbed rhodamine-tagged PEG after 6 h of UV exposure or the dark control.

10. Attenuated total reflectance – Fourier transform infrared (ATR-FTIR) spectroscopy

ATR-FTIR spectra were collected using a Nicolet Spectra 750 FTIR spectrometer equipped with a MIRacle ATR accessory (Pike Technologies, Madison, WI); 250 scans were collected at a resolution of 2 cm^{-1}. Sample was prepared for *in situ* exposure by first concentrating 500 µL of the stock cit-Au NPs (≈ 56 mg L^{-1} Au) to (5-10) µL in a pre-rinsed Protein LoBind microcentrifuge tube (Eppendorf, Hauppauge, NY), depositing the concentrated suspension onto a diamond ATR-FTIR crystal, and allowing the film to dry overnight within the spectrometer compartment. Then, 100 µL of 1 g L^{-1} $mPEGSH_{5000}$ solution was pipetted to cover the NP film, and spectra were recorded over 60 min until no further increase in ether absorbance was observed. The mPEGSH-coated AuNP film shows a strong absorbance at 1107 cm^{-1} characteristic of the C-O stretching bond in the PEG ether groups. Additional absorbance peaks are observed that have previously been assigned to the ether CH_2 groups of PEG, including the peaks near 1350 cm^{-1} (wagging mode), (948 and 850) cm^{-1} (rocking modes), and (1300 and 1250) cm^{-1} (twisting modes).[4, 5]

The polymer solution was removed by wicking with a cotton swab, and the film was rinsed by several depositions and wicking of 50 µL aliquots of DI H_2O, followed by a final deposition of 50 µL of DI H_2O and placement of a quartz coverslip with petroleum jelly seal. Minimal loss of the ether absorbance peak was observed during the rinsing procedure (Figure S3a). The last spectrum collected after placement of the quartz coverslip was used as the background spectrum to obtain difference spectra upon UV exposure.

UV exposure was performed outside of the FTIR instrument using a Spectroline UV-4AW single-lamp unit (Westbury, NY), using the same lamp (RMR-3500A, Southern New England Ultraviolet Co., Branford, CT) as in the Rayonet reactor. The lamp was held ≈ 5 cm above the crystal; the irradiance measured by top-down exposure of ferrioxalate solutions in open glass vials was 70 W m^{-2}. The difference spectra collected after (3 and 24) h of UV exposure suggest progressive loss of ether groups (Figure S3b). A significant limitation in the FTIR analysis is the uncertainty in the stability of the mPEGSH-coated AuNP film against desorption from the diamond surface. This uncertainty is compounded by the progressive baseline tilting observed over time (which may arise from rearrangement of AuNPs on the diamond surface) and the lack of observation of new absorbance peaks for reaction products (e.g., ester or carboxyl) that could support a specific mechanism of PEG degradation, e.g., ether oxidation.

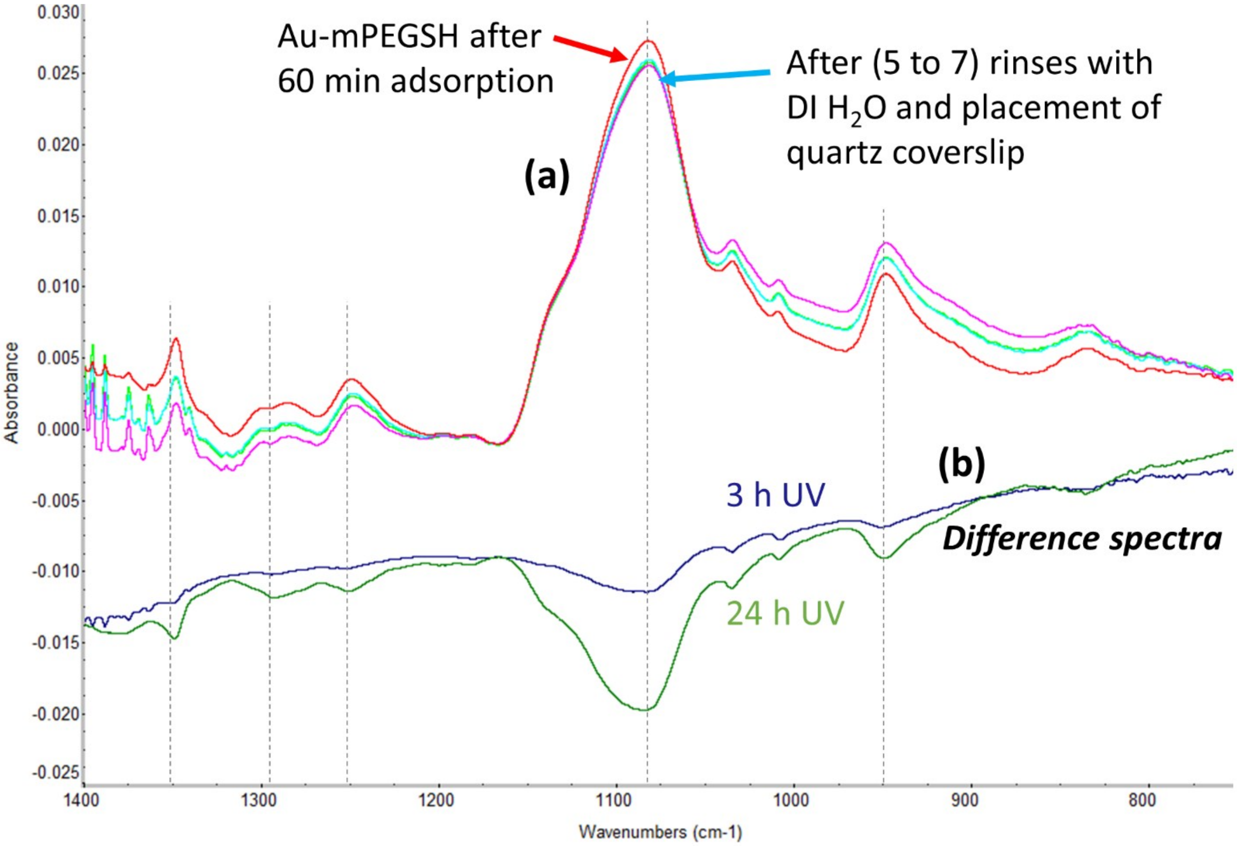

Figure S3. ATR-FTIR spectra for the $mPEGSH_{5000}$ coating on a Au NP film under liquid H_2O, after adsorption, rinsing, and placement of a quartz coverslip (a), followed by UV exposure (b). Spectra in (a) are referenced to the background spectrum of the cit-Au NP film under a 50 μL drop of DI H_2O prior to mPEGSH coating. Difference spectra in (b) are referenced to the last spectrum collected after placement of the quartz coverslip in (a). Spectra are shown on a common absorbance scale but have been vertically shifted for clarity.

11. XPS spectra for the washed, Au-mPEGSH NPs in DI water, ***prepared from partially oxidized mPEGSH stock***

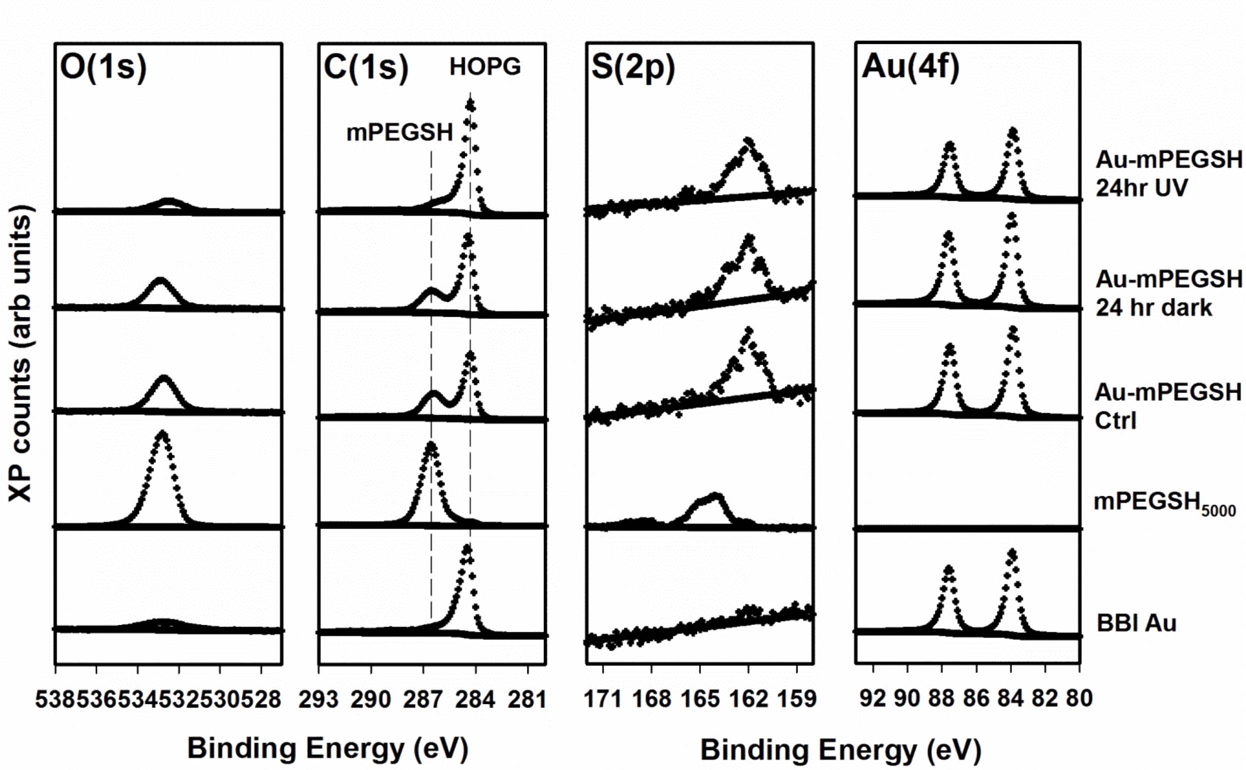

Figure S4. Representative spectra of the data presented in Figure 4 from the main text. "Au-mPEGSH Ctrl" denotes the as-prepared Au-mPEGSH NPs, and "BBI Au" denotes the citrate-stabilized AuNPs prior to PEGylation.

12. XPS results for the washed, Au-mPEGSH NPs in DI water, ***prepared from mPEGSH stock with dithiothreitol (DTT) impurity***

XPS results demonstrate that, even with DTT present in the mPEGSH_{5000} coating, the S:Au ratio does not change significantly in the present of UV radiation over a 24 h period. After 7 d, there was some evidence of loss in sulfur contributions. Figure S6 provides representative spectra for the samples analyzed.

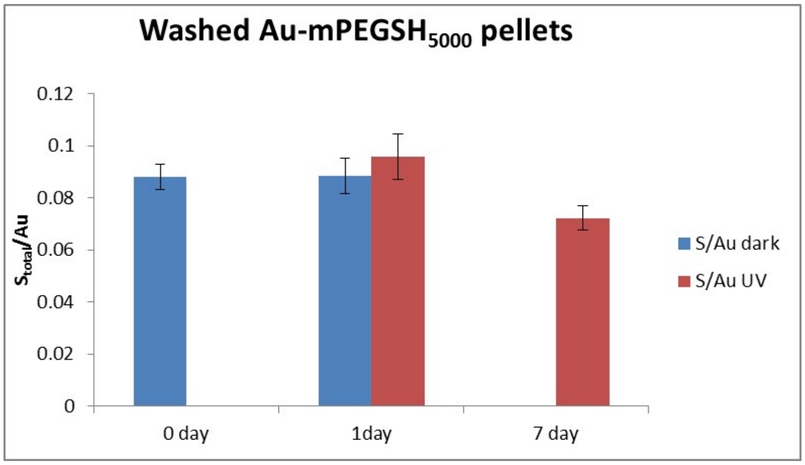

Figure S5. XPS derived ratios of total S to the Au surface concentration for washed Au-mPEGSH$_{5000}$ NPs (with DTT impurity) before and after UV irradiation in addition to one dark control. Values plotted are the average ± one standard deviation of at least three measurements.

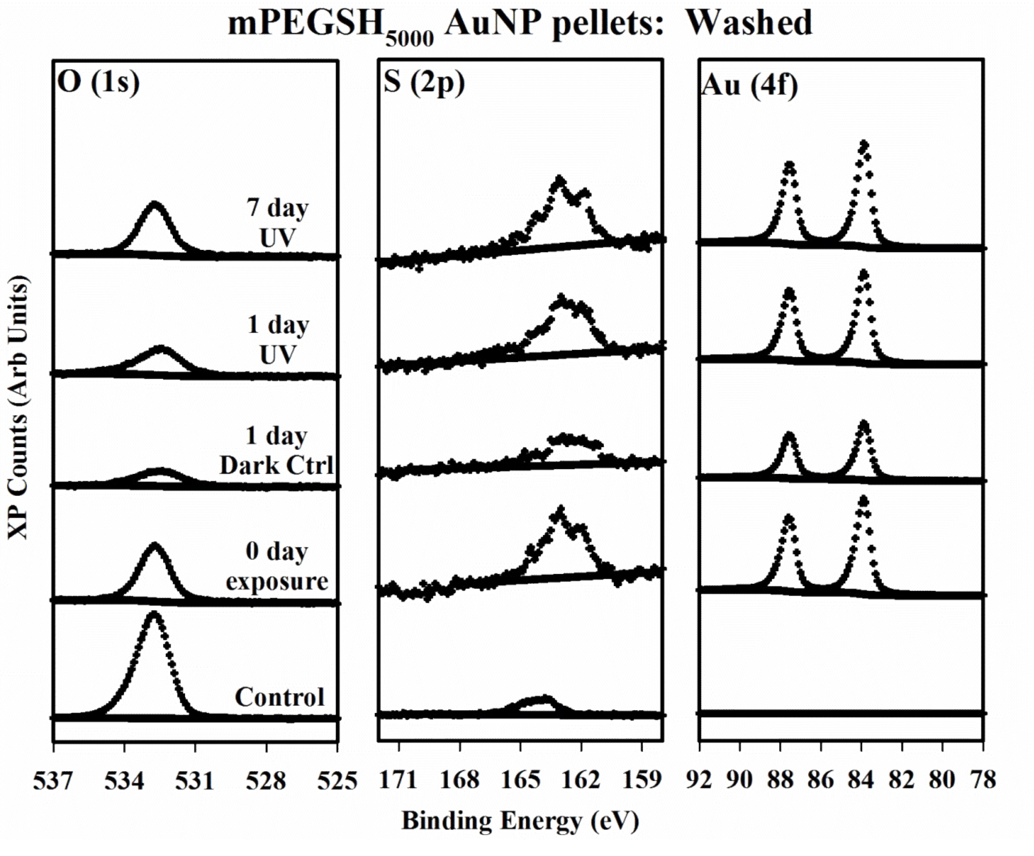

Figure S6. XPS stack plots of the centrifuged AuNP pellets prepared using the mPEGSH$_{5000}$ stock with DTT impurity. Spectral profiles of the S (2p) region suggest that all surface S species were not oxidized and either reside at the AuNP surface as either thiol or in an otherwise reduced form (*e.g.* thiolate). O (1s) spectra are presented to demonstrate that it was not possible to discern if PEG was removed or not by XPS for the DTT-containing coatings. "Control" refers to the mPEGSH$_{5000}$ stock (without NPs).

13. Aggregation in monovalent electrolyte solution (100 mmol L^{-1} NaCl with 0.9 mmol L^{-1} NaHCO$_3$, pH 8)

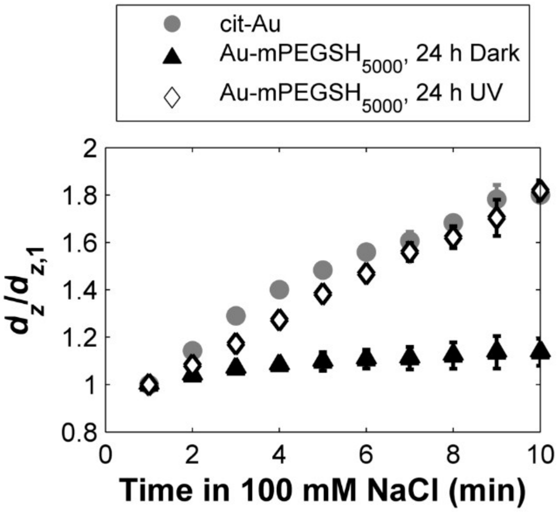

Figure S7. Time-resolved DLS measurements show that aggregation of the Au-mPEGSH$_{\mathbf{5000}}$ NPs in 100 mmol L$^{\mathbf{-1}}$ NaCl is minimal for the 24 h dark controls but near that of the cit-Au NPs after 24 h of UV irradiation. Au-mPEGSH$_{5000}$ NPs were prepared using the more highly reduced mPEGSH stock (with DTT impurity).

14. LC-MS: Proposed speciation of carbocation fragments and additional mass spectra

Table S4. Proposed speciation of fragments with *m*/*z* < 450

m/*z*	Proposed speciation
44.026*n* + 15 (e.g., 59, 103, …)	Methyl-terminated PEG carbocation fragment $H_3C(OCH_2CH_2)_n^+$
44.026*n* + 1 (e.g., 45, 89, 133, …)	Mid-chain PEG carbocation fragment $H(OCH_2CH_2)_n^+$
44.026*n* + 257.9 (e.g., 258, 302, 346, …)	TNB-derivatized PEG carbocation fragment (only observed during elution of derivatized mPEGSH; not observed in disulfide peak or in underivatized mPEGSH) 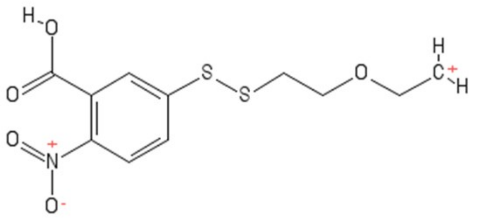

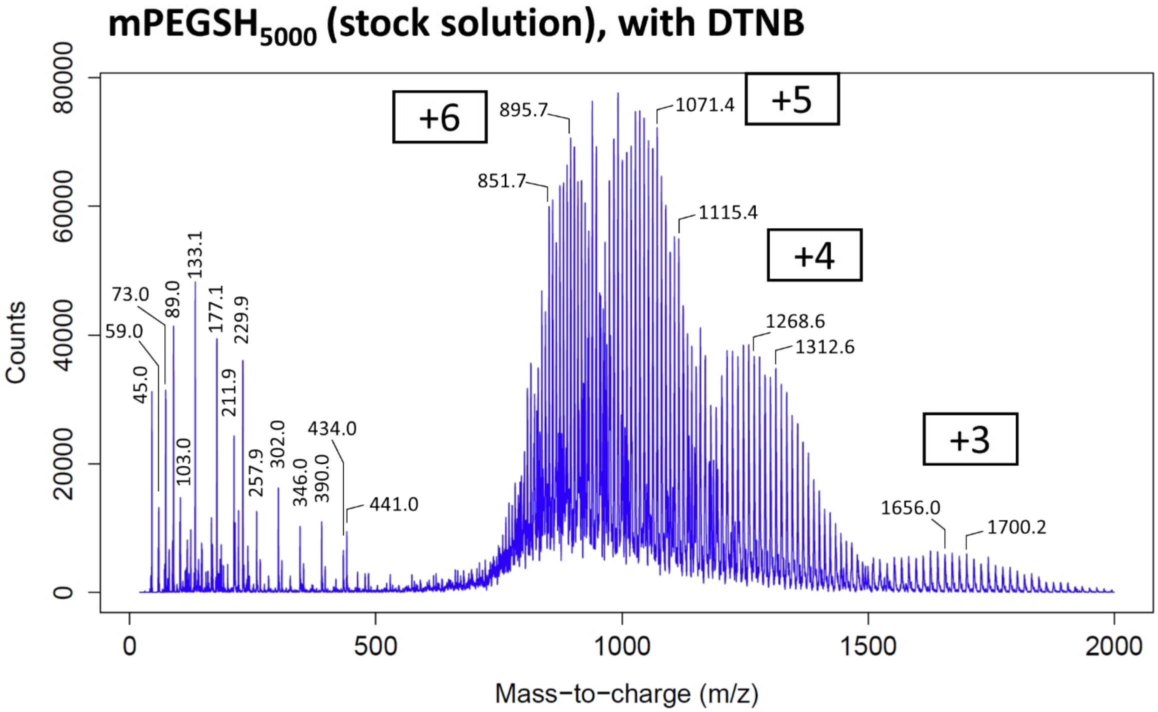

Figure S8. Mass spectrum for the stock mPEGSH$_{5000}$ (100 mg L^{-1}) after reaction with DTNB. The *m*/*z* distribution is consistent with a molar mass distribution centered near the expected value of 5 kDa. Sample was prepared from the mPEGSH stock containing DTT impurity.

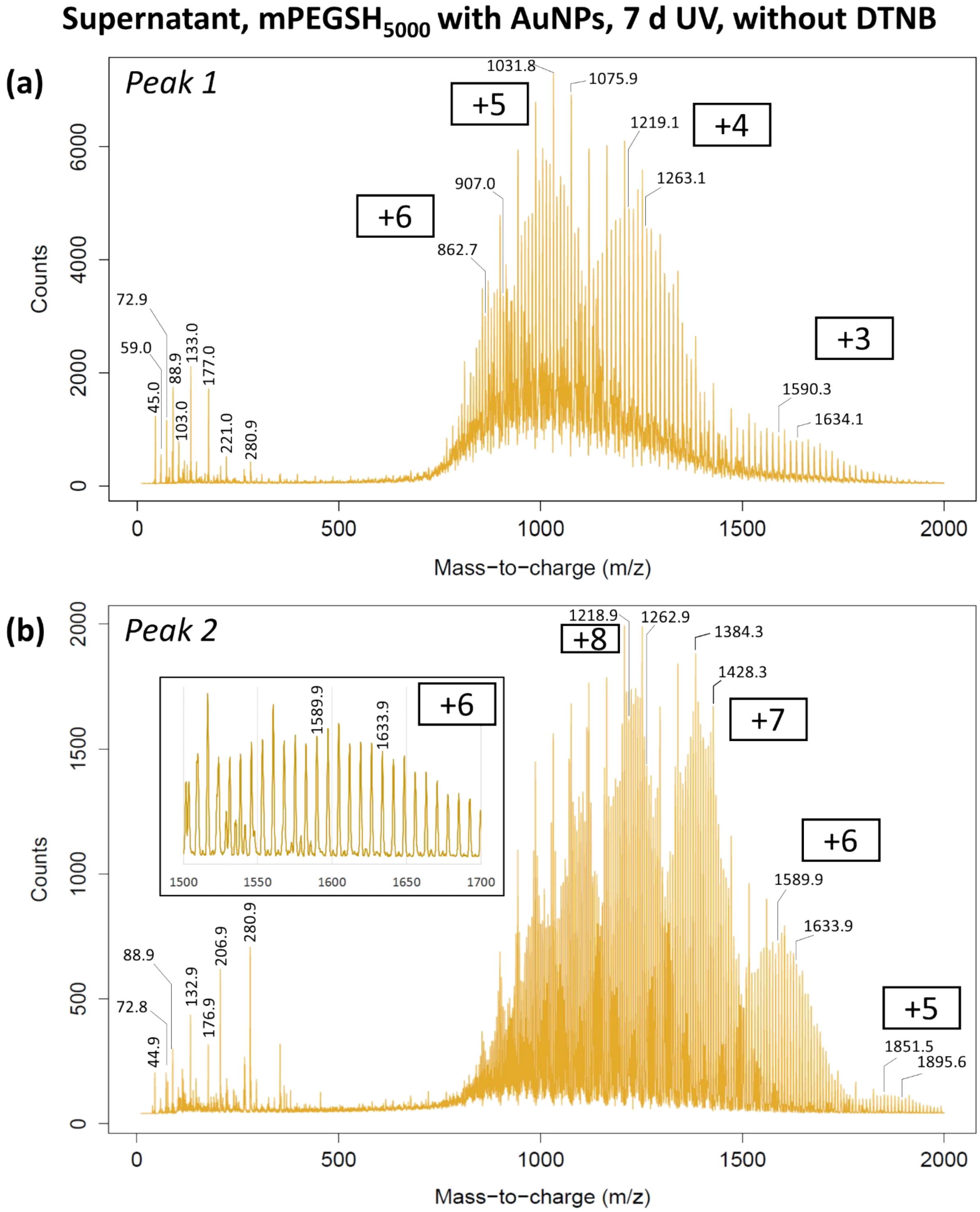

Supernatant, mPEGSH$_{5000}$ with AuNPs, 7 d UV, without DTNB

Figure S9. Mass spectra for mPEGSH$_{5000}$ supernatant collected after 7 d UV exposure in the presence of Au-mPEGSH$_{5000}$ NPs, without DTNB derivatization. (a) Thiols and (b) disulfides are observed. The inset in (b) expands the spectrum in the +6 charge state. Results are similar to the DTNB-derivatized sample (Figure 7 in main text) but with fewer species observed in the region of *m*/*z* < 700 Da. Sample was prepared from the mPEGSH stock containing DTT impurity.

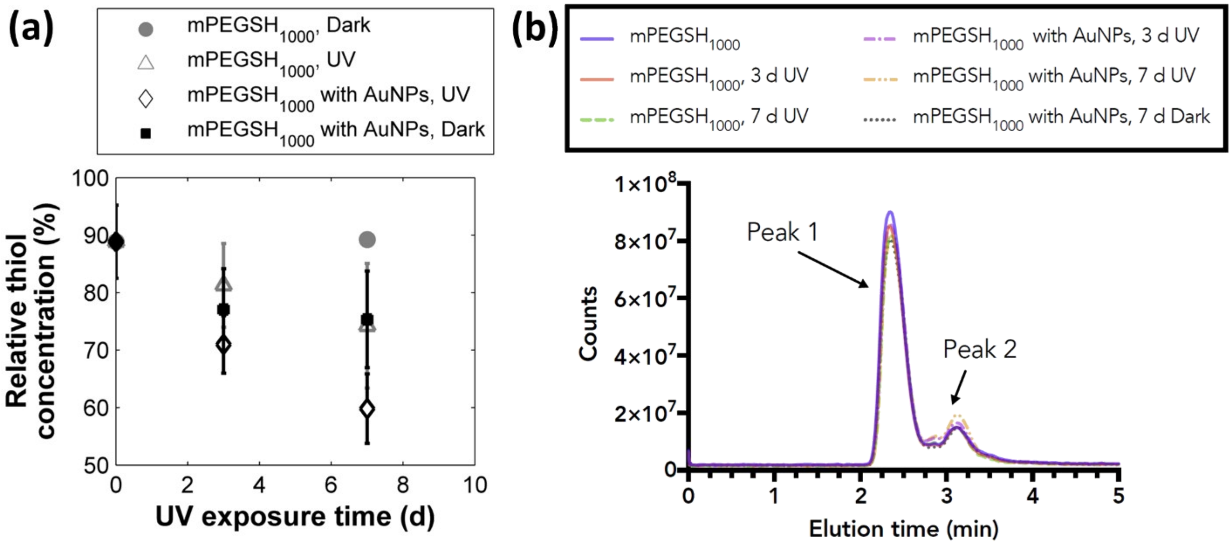

Figure S10. (a) Ellman's assay and (b) LC-MS chromatograms for mPEGSH$_{1000}$ solutions show a less significant effect of the UV-irradiated AuNPs on the rate of thiol loss in solution than for mPEGSH$_{5000}$. "mPEGSH$_{1000}$ with AuNPs" in the legends denotes the supernatant containing ≈ 100 mg L^{-1} of mPEGSH$_{1000}$ after pelleting the AuNPs by centrifugation. In (a), relative thiol concentrations are calculated from the measured absolute molar concentrations as a percentage of the nominal initial molar concentrations (100 μmol L^{-1}); error bars represent one standard deviation of measurements on five independent samples. Sample was prepared from the mPEGSH$_{1000}$ stock containing DTT impurity, and samples for LC-MS were reacted with DTNB immediately after collection.

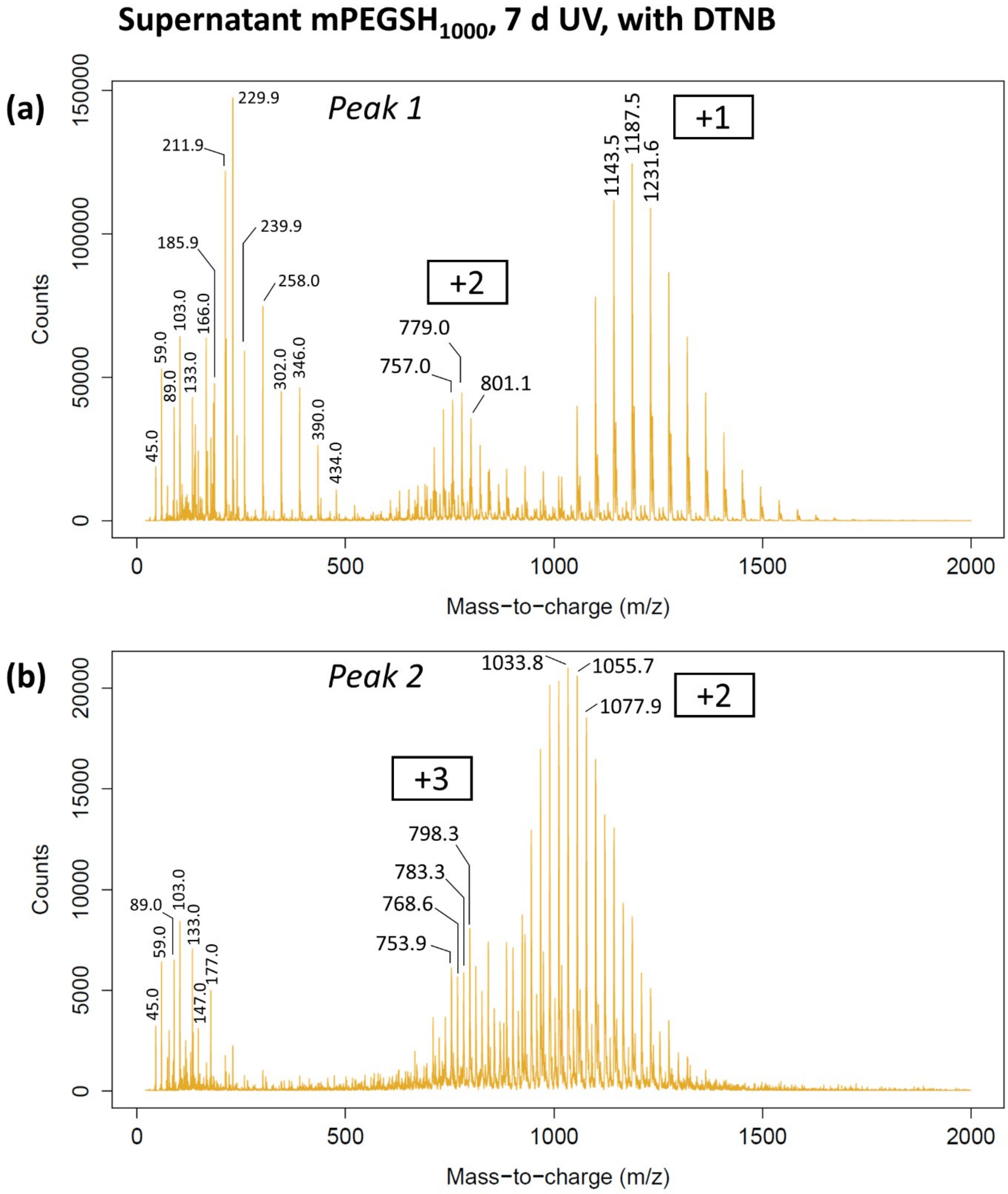

Figure S11. Mass spectra for mPEGSH$_{1000}$ supernatant collected after 7 d UV exposure in the presence of Au-mPEGSH$_{1000}$ NPs. mPEGSH$_{1000}$ exhibits less convoluted mass spectra than mPEGSH$_{5000}$. As for mPEGSH$_{5000}$, primarily (a) thiols and (b) disulfides were observed, with no evidence of significant chain scission compared to control mPEGSH$_{1000}$ solutions (not shown). Measured *m*/*z* values agree with calculated values for NH_4^+ adducts of the thiol or disulfide species within 0.1 u. Comparison against mass spectra for samples without TNB tagging (not shown) also confirmed the assignment of (a) to thiols and (b) to disulfides. Sample was prepared from the mPEGSH$_{1000}$ stock containing DTT impurity.

15. Total organic carbon analysis

Total organic carbon (TOC) was measured for the supernatants obtained from the Au-mPEGSH$_{5000}$ in 100 mg L^{-1} mPEGSH$_{5000}$ after 7 d of UV irradiation and the 7 d dark control. TOC measurements were collected on a Phoenix 8000 instrument (Teledyne Tekmar, Mason, OH). The default instrument method for TOC concentrations of (0.1 to 20) mg L^{-1} as C was used: 4.0 mL of sample was mixed with 0.5 mL of 21% phosphoric acid reagent and sparged with N_2 for 120 s to remove inorganic carbon; then, the sample and 1.0 mL of 10% persulfate/5% phosphoric acid reagent were injected into a UV reactor and sparged with N_2. CO_2 from oxidation of the organic carbon was monitored by a nondispersive infrared (NDIR) reactor. Calibration standards were prepared using mPEGSH$_{5000}$ solutions. No significant loss of carbon was observed in either the UV-irradiated or dark samples.

16. DLS measurements for Au-mPEGSH in solutions containing excess mPEGSH

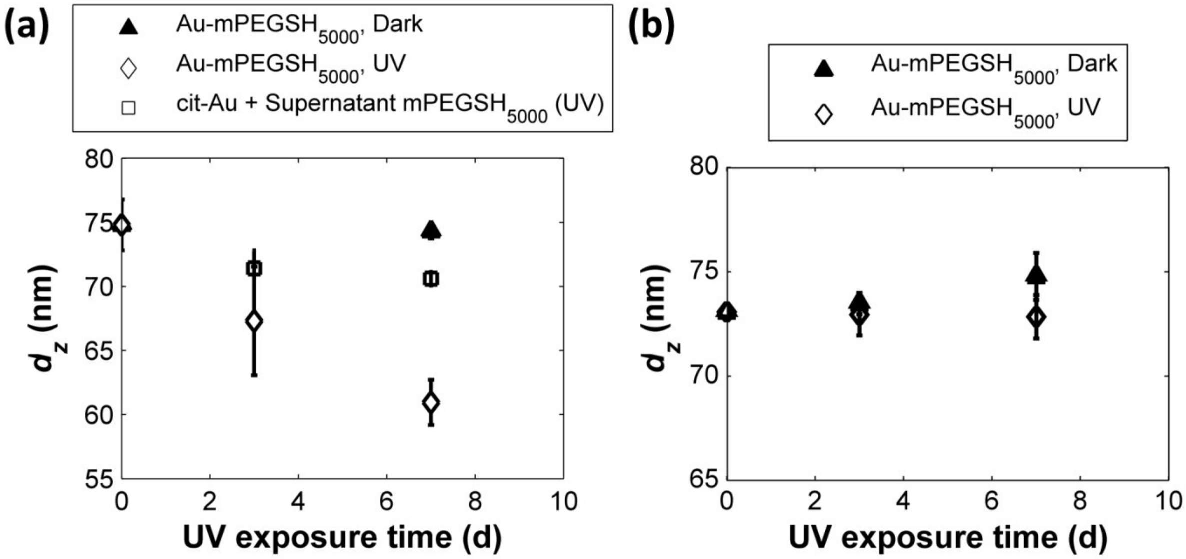

Figure S12. DLS measurements for Au-mPEGSH NPs in solutions of 100 mg L^{-1} mPEGSH, for (a) the partially oxidized mPEGSH (initial thiol concentration ≈ 7 μmol L^{-1}) or (b) the mPEGSH with DTT impurity (initial thiol concentration ≈ 20 μmol L^{-1}). Error bars represent one standard deviation of duplicate (a) and triplicate (b) measurements on independently prepared samples. In (a), dissolved polymer that was collected in the supernatant of the pelleted, UV-exposed NPs could still adsorb appreciably to fresh cit-AuNPs (empty squares), suggesting that the decrease in d_z observed for the UV-exposed Au-mPEGSH NPs is attributable to blocking of mPEGSH re-sorption by the transformed polymer coating. While the dissolved DTT impurity in (b) may be able to adsorb to the NP surface, the DLS data do not show a decrease in the mPEGSH layer thickness, suggesting little displacement of polymer by DTT (where only partial displacement of mPEGSH in high concentrations of DTT has previously been shown[6]) or preferential oxidation of dissolved DTT during the UV exposure.

17. Effects of inorganic solutes on the rate of coating transformation

Au-mPEGSH$_{5000}$ transformations were monitored in the presence of NO_3^- (from $NaNO_3$), H_2O_2, and $NaHCO_3$ (Figure S13). $HO^\bullet$ production rates were estimated from the spectral distribution of photon flux of the UV lamps and the absorbance spectra and quantum yield previously reported for H_2O_2,[7, 8] NO_3^-,[9] and NO_2^-.[9] The $HO^\bullet$ production rate (normalized by the surface area of irradiation) for the 0.1 mmol L^{-1} concentration of H_2O_2 is estimated to be 1.1×10^{-13} mol s^{-1} cm^{-2}. To obtain an equivalent $HO^\bullet$ production rate from NO_3^- or NO_2^-, estimated concentrations of ≈ 1.6 mmol L^{-1} (≈ 100 mg L^{-1}) for NO_3^- and 10 µmol L^{-1} (≈ 0.5 mg L^{-1}) for NO_2^- would be required, which are higher than environmentally relevant concentrations, e.g. < 2 mg L^{-1} total NO_3^- + NO_2^- as N (with NO_2^- generally making up < 1 % of the total) measured in a New Jersey watershed with nutrient loading primarily from non-point sources.[10]

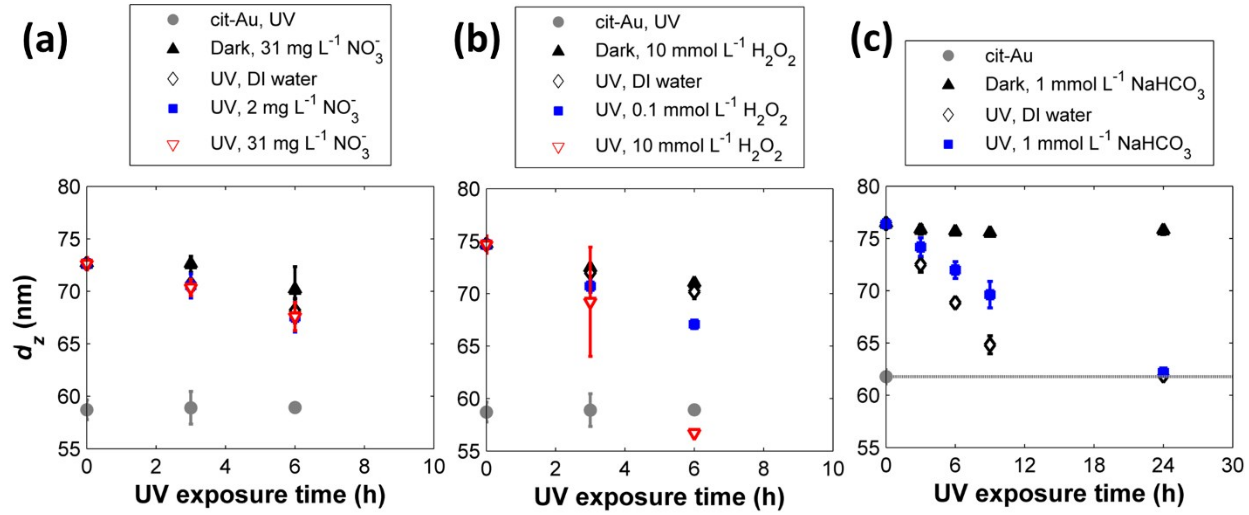

Figure S13. Transformations in $\boldsymbol{d_z}$ for UV-exposed and dark control Au-mPEGSH$_{\mathbf{5000}}$ NPs in the presence of (a) NO_3^-, (b) H_2O_2, and (c) $NaHCO_3$. The cit-Au NPs and Au-mPEGSH$_{5000}$ NPs in DI water are also shown for comparison. No significant effect is observed for NO_3^- compared to DI water under UV irradiation, whereas H_2O_2 accelerated the rate of coating loss and $NaHCO_3$ decreased the rate of coating loss. Values plotted represent the average and standard deviation of duplicate runs, except in (c) for "UV, DI water" and cit-Au (average and standard deviation of five measurements for a single experiment). Note cit-Au size differs in (c) compared to (a) and (b) because a different batch of NPs was used. Au-mPEGSH NPs were prepared using the more highly reduced mPEGSH stock (with DTT impurity).

References

1. E. Fischer, *EPA Newsletter*, 1984, **21**, 33-34.
2. T. J. Cho, J. M. Pettibone, J. M. Gorham, T. M. Nguyen, R. I. MacCuspie, J. Gigault and V. A. Hackley, *Langmuir*, 2015, **31**, 7673-7683.
3. A. V. Naumkin, A. K. Kraut-Vass, S. W. Garenstroom and C. J. Powell, in *NIST Standard Reference Database 20, Version 4.1*, National Institute of Standards and Technology, 2012.
4. P. Harder, M. Grunze, R. Dahint, G. M. Whitesides and P. E. Laibinis, *J Phys Chem B*, 1998, **102**, 426-436.
5. Y. Kuroda and M. Kubo, *J. Polym. Sci.*, 1957, **26**, 323-328.
6. D.-H. Tsai, M. P. Shelton, F. W. DelRio, S. Elzey, S. Guha, M. R. Zachariah and V. A. Hackley, *Anal. Bioanal. Chem.*, **404**, 3015-3023.
7. R. F. Beers and I. W. Sizer, *J Biol Chem*, 1952, **195**, 133-140.
8. S. Goldstein, D. Aschengrau, Y. Diamant and J. Rabani, *Environ. Sci. Technol.*, 2007, **41**, 7486-7490.
9. J. J. Jankowski, D. J. Kieber and K. Mopper, *Photochem Photobiol*, 1999, **70**, 319-328.
10. C. M. Weiben, R. J. Baker and R. S. Nicholson, *Nutrient concentrations in surface water and groundwater, and nitrate source identification using stable isotope analysis, in the Barnegat Bay-Little Egg Harbor Watershed, New Jersey, 2010–11*, Report U.S. Geological Survey Scientific Investigations Report 2012-5287, 2013.